Front. Environ. Sci. Eng. 2014, 8(3): 463–470
DOI 10.1007/s11783-013-0575-3

RESEARCH ARTICLE

Cation exchange resin supported nanoscale zero-valent iron for removal of phosphorus in rainwater runoff

Bangmi XIE, Jiane ZUO (✉), Lili GAN, Fenglin LIU, Kaijun WANG

State Key Joint Laboratory of Environment Simulation and Pollution Control, School of Environment, Tsinghua University, Beijing 100084, China

Abstract Self-made cation exchange resin supported nanoscale zero-valent iron (R-nZVI) was used to remove phosphorus in rainwater runoff. 80% of phosphorus in rainwater runoff from grassland was removed with an initial concentration of 0.72 $mg \cdot L^{-1}$ phosphorus when the dosage of R-nZVI is 8 g per liter rainwater, while only 26% of phosphorus was removed when using cation exchange resin without supported nanoscale zero-valent iron under the same condition. The adsorption capacity of R-nZVI increased up to 185 times of that of the cation exchange resin at a saturated equilibrium phosphorous concentration of 0.42 $mg \cdot L^{-1}$. Various techniques were implemented to characterize the R-nZVI and explore the mechanism of its removal of phosphate. Scanning electron microscopy (SEM) indicated that new crystal had been formed on the surface of R-nZVI. The result from inductive coupled plasma (ICP) indicated that 2.1% of nZVI was loaded on the support material. The specific surface area was increased after the load of nanoscale zero-valent iron (nZVI), according to the measurement of BET-N_2 method. The result of specific surface area analysis also proved that phosphorus was removed mainly through chemical adsorption process. X-ray photoelectron spectroscopy (XPS) analysis showed that the new product obtained from chemical reaction between phosphate and iron was ferrous phosphate.

Keywords nanoscale zero-valent iron(R-nZVI), cation exchange resin, rainwater runoff, phosphorus adsorption

1 Introduction

With the urbanization accelerated recently, impervious area in the urban area increased rapidly and the emission of non-point source pollutants increased simultaneously, among which the non-point pollution coming from rainwater runoff became more and more serious. If untreated rainwater runoff is directly discharged into the urban water body, severe eutrophication problem will be caused. Main pollutants in rainwater runoff are organics, suspended solid, nitrogen and phosphorus. According to the study of a Canadian research group (Experimenta1 Lake Area, ELA) [1], phosphorus was the controlling factor for eutrophication in most lakes. Chinese researchers have also demonstrated that the eutrophication of several Chinese main lakes such as Taihu Lake and Dongting Lake is controlled by phosphorus rather than nitrogen. Currently the accepted Total phosphorus (TP) concentration threshold for eutrophication is 0.02 $mg \cdot L^{-1}$ [2]. However, researchers showed that in Beijing, the average TP concentration in rainwater runoff was 1.74 $mg.L^{-1}$ which was much higher than the threshold [3]. So, a proper treatment process is needed to remove phosphorus from rainwater runoff before it is discharged into the water body. Due to the limitation of urban area and the low concentration of phosphorus, rainwater infiltration pond becomes one of the most common methods to treat rainwater runoff due to its simple technical process, convenient management, flexible design, etc. The phosphorus in rainwater runoff is presented mainly in particulate form, but the dissolved phosphorus concentration is sometimes relatively very high. The particulate phosphorus can be removed by filtration easily, so more attention is focused on the removal of dissolved phosphorus which depends mainly on the adsorption capacity of the filter media in the infiltration pond. In the previous study of our group's, 12 common materials, such as activated carbon, anthracite, quartz sand, etc., were studied, and some were chosen as the filtration media for rainwater infiltration pond. However, the adsorption capacities of these materials were highly limited and

Received March 28, 2013; accepted July 28, 2013

E-mail: jiane.zuo@tsinghua.edu.cn

most of them would be saturated by the phosphorus in the rainwater runoff within one year [4]. Therefore, materials with higher phosphorus adsorption capacities are necessary to be developed for engineering application.

There are two ways to meet this goal. One is to increase the specific surface area of the absorbents, and the other is to improve the reactivity of the absorbents. The application of nanoscale zero-valent iron (nZVI) is a better approach which combines these two ways together. Due to its nanoscale dimensions, nZVI particles have a large specific surface area which provides more active sites than conventional microscale materials for pollutant removal [5], meanwhile, the activity of reaction with phosphate could be improved since phosphate salts can be easily reacted with iron.

nZVI has been extensively investigated in numerous studies for the remediation of polluted water, and it has been proven very high efficient for treating organic and inorganic pollutants [6]. It has been demonstrated that nZVI can remove metallic and nonmetallic pollutants, including chlorinated organics, organic dyestuffs, heavy metal ions and inorganic negative ions, existed in different types of soil and water [6,7]. But it's rarely reported that nZVI is directly used to remove phosphorus in rainwater runoff. Meanwhile, there are several potential limitations which limit the applications of nZVI. For example, due to their nano-scale size, they are easily to be washed out when they are applied in the systems such as infiltration tanks, and they can inevitably cause high pressure drops in conventional filtration systems [8].

In this paper, self-synthesized nZVI was loaded on resin as a supported material. Phosphorus removal efficiency and adsorption capacities of R-nZVI were calculated and compared with the raw material. Synthesized R-nZVI was characterized using scanning electron microscopy (SEM), inductive coupled plasma (ICP) and BET-N_2 adsorption technique. X-ray photoelectron spectroscopy (XPS) was implemented to try to explain the mechanism for the removal of phosphate with nZVI.

2 Materials and methods

2.1 Materials

All chemicals were analytical grade reagents with no further purification, including potassium borohydride (KBH_4), ferrous sulfate heptahydrate ($FeSO_4 \cdot 7H_2O$), ethanol (C_2H_6O), monopotassium phosphate (KH_2PO_4), sodium hydroxide (NaOH), hydrochloric acid (HCl).

Strong acid cation exchange resin (styrene; exchange capacity ($mmol \cdot g^{-1}$ (dry resin) $\geqslant$ 4.2 (Na^+); grain size (0.3–1.2 mm) $\geqslant$ 95%; moisture content: 46%–52%) was bought from Sinopharm Chemical Reagent Co., LTD.

Rainwater runoff was collected from the surface of a lawn on campus of Tsinghua University, Beijing, China. The concentration of dissolved phosphorus was around $0.7\ mg \cdot L^{-1}$.

2.2 Preparation of R-nZVI

First, the resin was treated in hydrochloric acid solution (HCl, $2\ mol \cdot L^{-1}$) for 30 min to exchange Na^+ into H^+. Then the resin was washed by de-ionized (DI) water three times to remove residual HCl. Secondly, 15 g resin (dry weight) was mixed with 200 mL ferrous sulfate solution (containing 3 g Fe) and was vigorously stirred for 2 h. After that the treated resin was washed by de-ionized water to remove residual Fe^{2+}. Thirdly, the treated resin was mixed in ethanol solution (30% (v/v water)) and 100 mL KBH_4 ($1.08\ mol \cdot L^{-1}$; pH = 12) solution was added to this mixture at a rate of 20–30 drops per minute while stirring continuously. After the mixture stopping releasing hydrogen, the prepared material was washed and dried in vacuum centrifugal concentrator (5301, Eppendorf, Germany) for 24 h. The reaction was processed as follow Eq. (1):

$$2Fe^{2+} + BH_4^- + 3H_2O \rightarrow 2Fe \downarrow + H_2BO_3^- + 4H^+ + 2H_2 \uparrow \quad (1)$$

2.3 Phosphorus adsorption experiment

Resin and R-nZVI were added into rainwater runoff in flasks with different dosage. The flasks were placed on a shaker ($150\ r \cdot min^{-1}$) at 25°C. The residual concentration of dissolved phosphorus in supernatant solutions was measured using malachite green-molybdophosphate method (Ministry of Environmental Protection of China, 2002) at certain reaction time intervals until the reaction system reached the state of adsorption equilibrium. The adsorption isotherms were plotted to calculate the adsorption capacity according to Langmuir Model or Freundich Model [9].

2.4 Characterization

The concentration of P in solution was determined by ultraviolet specrophotometer (DR2800, Hach, USA). Scanning electron microscope (SEM) images of resin and R-nZVI, recorded at different magnifications, were observed on a scanning electron microscope (S5500, Hitachi, Japan) operating at 5 kV. The specific surface areas were measured by a N_2 adsorption surface area and pore size analyzer (QuadraSorb SI, Quantachrome, USA) according to the standard GB/T 19587–2004. The amount of Fe loaded onto resin was determined by inductive coupled plasma (ICP) (IRIS Intrepid II XSP, Thermo Fisher, USA) after being dissolved by H_2SO_4 solution. The X-ray photoelectron spectroscopy (XPS) analysis of the surface composition and the elements' valence was carried out on an X-ray photoelectron spectroscopy (ESCALAB

250Xi, Thermo, UK). The calibration of the binding energy of the spectra was achieved with aliphatic adventitious hydrocarbons C 1s peak at 284.6 eV.

3 Results and discussion

3.1 Characterization of the materials

The result from ICP showed that no iron was contained in bare resin while 2.1% (mass fraction) of iron was loaded onto R-nZVI. Compared with resin, the specific surface area of R-nZVI measured by a BET-N_2 surface area analyzer was increased from 0 to 0.13 $m^2 \cdot g^{-1}$, when 2.1% of nZVI was loaded onto resin. The SEM images of resin and R-nZVI were shown in Fig. 1. Before loaded with nZVI, the surface of resin was smooth and compact, as shown in Figs. 1 (a) and 1(c). The compact structure explained the small specific surface area of resin. Figures 1 (b) and 1(d) showed the surface image of R-nZVI, which became rather rough, and some amorphous iron was found on the surface. The loose surface structure and the small sized iron particles on the surface made the specific surface area of R-nZVI increased greatly.

3.2 Removal of dissolved phosphorus in rainwater runoff

The removal efficiencies of resin and R-nZVI for dissolved phosphorus in rainwater runoff are shown in Table 1. 80% of phosphorus was removed from rainwater with the dosage of 8 g R-nZVI for one liter rainwater. In contrast, only 26% of phosphorus was removed when using the bare resin without supported nZVI at the same condition. This indicated that nZVI played a major role for the removal of

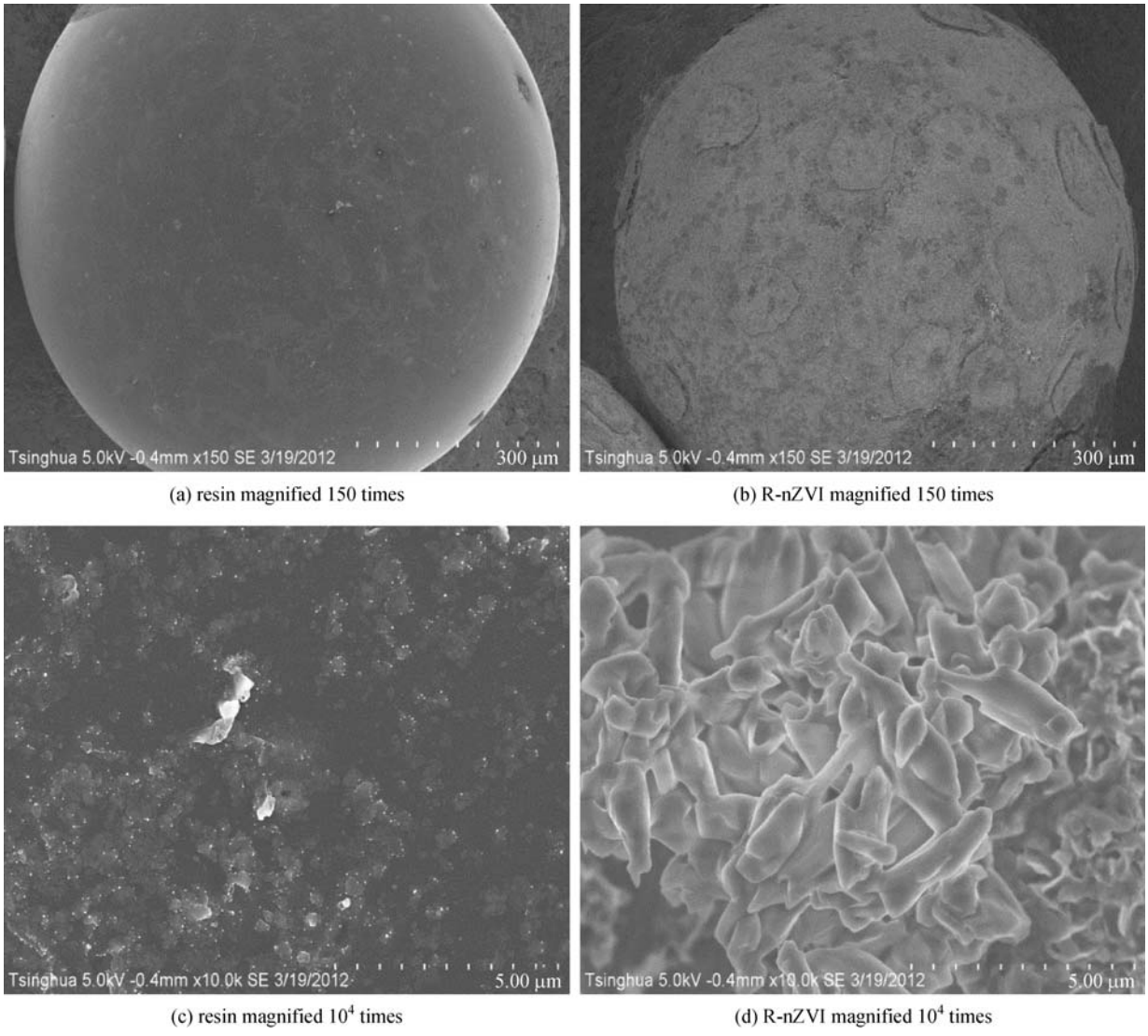

(a) resin magnified 150 times

(b) R-nZVI magnified 150 times

(c) resin magnified 10^4 times

(d) R-nZVI magnified 10^4 times

Fig. 1 SEM images of bare resin and R-nZVI. (a) resin magnified 150 times, (b) R-nZVI magnified 150 times, (c) resin magnified 10^4 times, (d) R-nZVI magnified 10^4 times

Table 1 Phosphorus removal efficiency of bare resin and R-nZVI

dosage/($g \cdot L^{-1}$)	1	2	4	8
efficiency of resin	14%	18%	21%	26%
efficiency of R-nZVI	66%	70%	76%	80%

phosphorus from rainwater runoff.

Freundlich model gave a better fit to the adsorption process than Langmuir Model. Fig. 2 showed the Freundlich isotherms for the adsorption on resin and R-nZVI ($R^2 > 0.98$). From the figure, the Freundlich equations for both R-nZVI and the bare resin could be derived, and were shown in the figure. According to the equations, the adsorption capacities (Q) at different equilibrium concentrations (C_e) could be calculated.

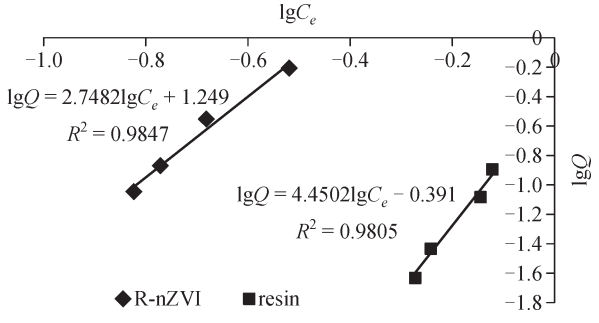

Fig. 2 Freundlich isotherms for the adsorption of dissolved phosphorus in rainwater runoff

The adsorption capacities of the bare resin and R-nZVI were shown in Table 2. Capacities of nZVI and nZVI modified zeolit studied in our previous studies were also included for comparison [10]. In the previous studies, rainwater runoffs were monitored in a Chinese city [4], and the annual average concentration of dissolved phosphorus was $0.42\ mg \cdot L^{-1}$, which made it reasonable to consider $0.42\ mg \cdot L^{-1}$ as the concentration of influent for an infiltration tank. In addition, according to fixed-bed adsorption theory, the adsorption media in an infiltration tank will reach its max adsorption capacity when the adsorption equilibrium concentration equals to the influent concentration [9]. Therefore, the concentration of $0.42\ mg \cdot L^{-1}$ was chosen as the equilibrium concentration to calculate the capacity in the case of the Chinese city.

Table 2 Adsorption capacities at the equilibrium concentration of $0.42\ mg \cdot L^{-1}$

adsorbent	capacity/($mg \cdot g^{-1}$)	capacity ratio to that of the bare resin
resin	0.009	1
R-nZVI	1.635	182
nZVI modified zeolite	0.604	67
nZVI	5.244	583

As shown in Table 2, compared with the bare resin, the adsorption capacity of R-nZVI for phosphorus increased from only $0.009\ mg \cdot g^{-1}$ to $1.635\ mg \cdot g^{-1}$, which was about 182 times compared with that of the bare resin. The capacity of R-nZVI was also increased compared with nZVI modified zeolit ($0.604\ mg \cdot g^{-1}$), which was synthesized in our previous study. The highest adsorption capacity was that of the pure nZVI, which was about 3.2 times of that of R-nZVI. However, according to the measurement result of ICP, only 0.021 g Fe was loaded on 1 g resin, therefore, based on per unit mass of Fe, the adsorption capacity of R-nZVI exceeded that of the pure nZVI up to $77.9\ mg \cdot g^{-1}$ Fe, which indicated that the reaction activity of nZVI loaded on the resin was improved significantly compared with the pure nZVI. One possible reason for this was that as a support material, resin could stabilize and disperse the nZVI particles as well as prevent nZVI from aggregation, which made the size of nZVI particles smaller [11]. The nZVI with smaller particle size would exhibit larger accessible surface areas and higher reactivity [12]. The results showed that synthesized R-nZVI could satisfy the requirement of engineering application, and could be used as the filtration media for rainwater infiltration pond, and due to its high adsorption capacity, there was no need to replace the material frequently.

Many other kinds of modified adsorption materials were also synthesized in other studies. For example, synthetic iron oxide coated sand, naturally iron oxide coated sand and iron oxide coated crushed brick were synthesized, and the maximum adsorption capacities for phosphorus of these materials were $1.5\ mg \cdot g^{-1}$, $1.8\ mg \cdot g^{-1}$ and $0.88\ mg \cdot g^{-1}$, respectively [13]. The modified zeolite was used to remove ammonium and phosphorus from the treated municipal wastewater, and the capacity for phosphorus adsorption reached $1.1\ mg \cdot g^{-1}$ when the equilibrium concentration was $0.42\ mg \cdot L^{-1}$ [14]. The R-nZVI synthesized in this study had a comparably better performance in the adsorption of phosphorus.

3.3 The mechanism of the phosphorus adsorption

The specific surface area of the R-nZVI was only $0.13\ m^2 \cdot g^{-1}$, while that of the pure nZVI in our previous study was $32.38\ m^2 \cdot g^{-1}$ [10]. Limited by the mass of iron loaded on the resin, the specific surface area of the R-nZVI was still very small. It was even smaller than those of some porous materials such as granular activated carbon, whose specific surface area can be up to more than $1000\ m^2 \cdot g^{-1}$. But its adsorption capacity was relatively very high. The results suggested that the removal of phosphorus was not a simple physical adsorption process, and the chemical adsorption process could have very big contribution to the high adsorption capacity.

XPS technique was employed to analyze the mechanism

for adsorption of phosphorus by nZVI and R-nZVI. Because the compounds in rainwater were too complex to analyze, the synthetic KH_2PO_4 solution was used to modify the adsorption process instead of the real collected rainwater.

Figure 3 showed a full survey of the surface chemical composition for the pure nZVI after adsorption. For the survey of Fe 2p core levels (Fig. 4(a)), the photoelectron peaks at 709.75 eV, 710.73 eV, 713.24 eV represented the binding energies of Fe(2p3/2),the peaks at 718.60 eV and 724.29 eV represented the binding energies of shake-up satellite 2p3/2 and 2p1/2. Peaks at 709.75 eV, 710.73 eV and 724.29 eV implied that Fe^0 particles were changed into iron oxides, in the form of FeO and Fe_2O_3 [15]. Fe_2O_3 proved to be the main oxidation product according to the comparison of peak area. The peak at 713.24 eV resulted from the iron bonding with P. In addition, the peak at 706.1 eV corresponding to zero-valent iron (Fe^0 2p3/2) [16] couldn't be observed within the detected length of XPS (less than 10 nm), which stated that Fe^0 on the surface was oxidized completely.

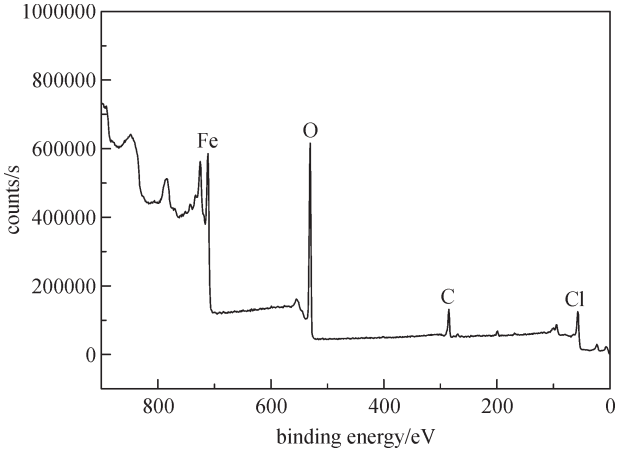

Fig. 3 XPS spectra of full survey of nZVI after adsorption

O 1s peak (Fig. 4(b)) appearing at 529.76 eV corresponded to the oxygen in FeO and Fe_2O_3. The peak at 531.00 eV corresponded to the oxygen in PO_4^{3-}. The product obtained from reaction between Fe and P could be shown by P 2p peak at 133.58 eV (Fig. 4(c)), which was the binding energy of P in iron phosphate.

Based on the analysis described above, the mechanism for removing PO_4^{3-} from aqueous solution by nZVI involved two strategies: the oxidation of Fe^0 to Fe^{3+} and the combination of Fe^{3+} and PO_4^{3-}, which precipitated in the form of iron phosphate. All the chemical reactions occurring were described as following Eqs. (2)–(5):

$$2Fe^0 + O_2 \rightarrow 2FeO \quad (2)$$

$$4Fe^0 + 3O_2 \rightarrow 2Fe_2O_3 \quad (3)$$

$$4Fe^0 + 3O_2 + 6H_2O \rightarrow 4Fe^{3+} + 12OH^- \quad (4)$$

$$Fe^{3+} + PO_4^{3-} \rightarrow FePO_4 \downarrow \quad (5)$$

Figure 5 showed a full survey of the surface composition for the R-nZVI after adsorption. The spectra of potassium implied that potassium existed in resin due to iron exchange. Majority of Fe existed in the form shown by Fe 2p peaks (Fig. 6(a)) at 712.06 eV and 725.87 eV, which represented the binging energy of Fe bond with sulfonyl in resin. The peak at 714.72 eV corresponded to the rest of Fe reacted with phosphate. O 1s peaks (Fig. 6(b)) at 530.89 eV and 532.21 eV resulted from oxygen in PO_4^{3-} and resin. For P 2p (Fig. 6(c)), the binding energy was 133.4 eV, which agreed with the value of ferrous phosphate according to the handbook of X-ray photoelectron spectroscopy.

Based on the results described above, the mechanism can also be explained by oxidation and precipitation. The chemical reactions involved were as following Eqs. (6)–(9):

$$R-SO_3^- + K^+ \rightarrow R-SO_3K \quad (6)$$

$$2Fe^0 + O_2 + 2H_2O \rightarrow 2Fe^{2+} + 4OH^- \quad (7)$$

$$2(R-SO_3^-) + Fe^{2+} \rightarrow (R-SO_3)_2Fe \quad (8)$$

$$3Fe^{2+} + 2PO_4^{3-} \rightarrow Fe_3(PO_4)_2 \downarrow \quad (9)$$

In conclusion, phosphate was removed mainly through chemical reaction, which was called chemical adsorption. XPS analyses indicated that iron phosphate was generated when nZVI was used to adsorb phosphate while ferrous phosphate was generated when R-nZVI was used.

4 Conclusions

Cation exchange resin-supported nanoscale zero-valent iron which contained 2.1% of nZVI was synthetized in this paper. The adsorption capacity of R-nZVI was greatly increased from 0.009 $mg \cdot g^{-1}$ to 1.585 $mg \cdot g^{-1}$ at a saturated equilibrium phosphorous concentration of 0.42 $mg \cdot L^{-1}$, which was 182 times of the bare resin. The nZVI supported on resin was more reactive and efficient than the pure nZVI, because the resin could prevent nZVI from aggregation and make the particle smaller. Phosphate was removed by nZVI mainly through chemical reactions and XPS analyses demonstrated that iron phosphate was produced when the pure nZVI was used to adsorb phosphate, while ferrous phosphate was produced when the R-nZVI was used.

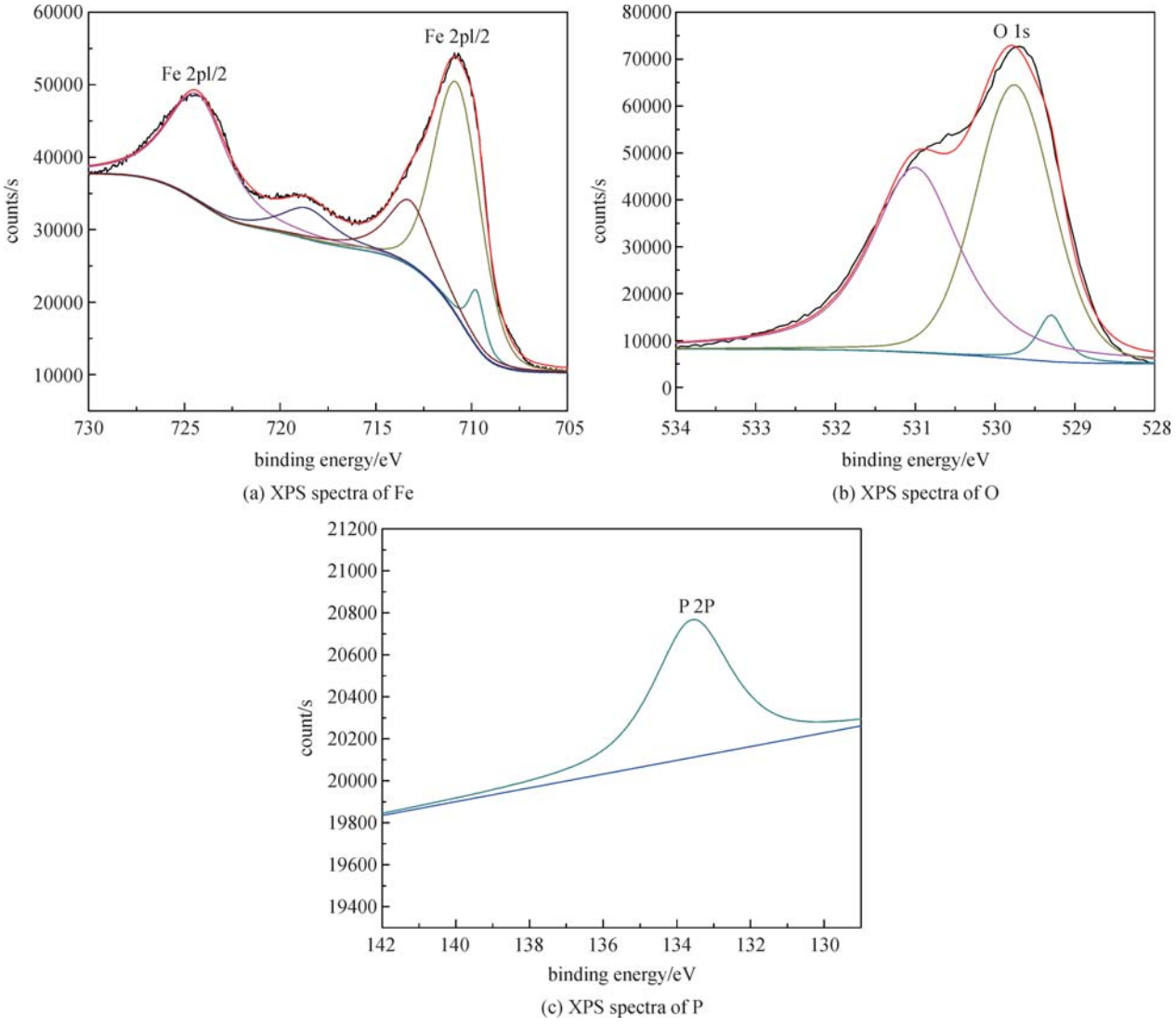

Fig. 4 XPS spectra of Fe, O, P, in nZVI after adsorption

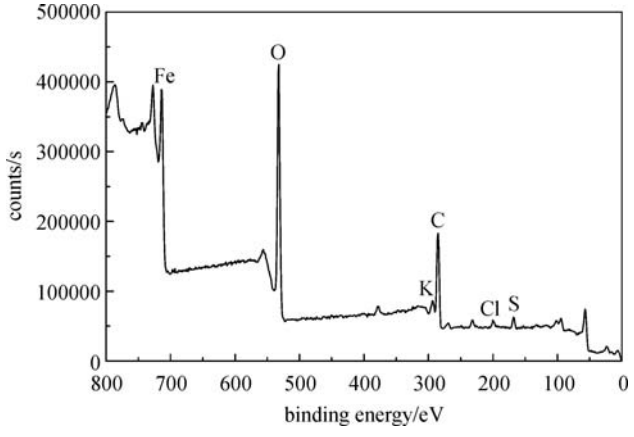

Fig. 5 XPS spectra of full survey of R-nZVI after adsorption

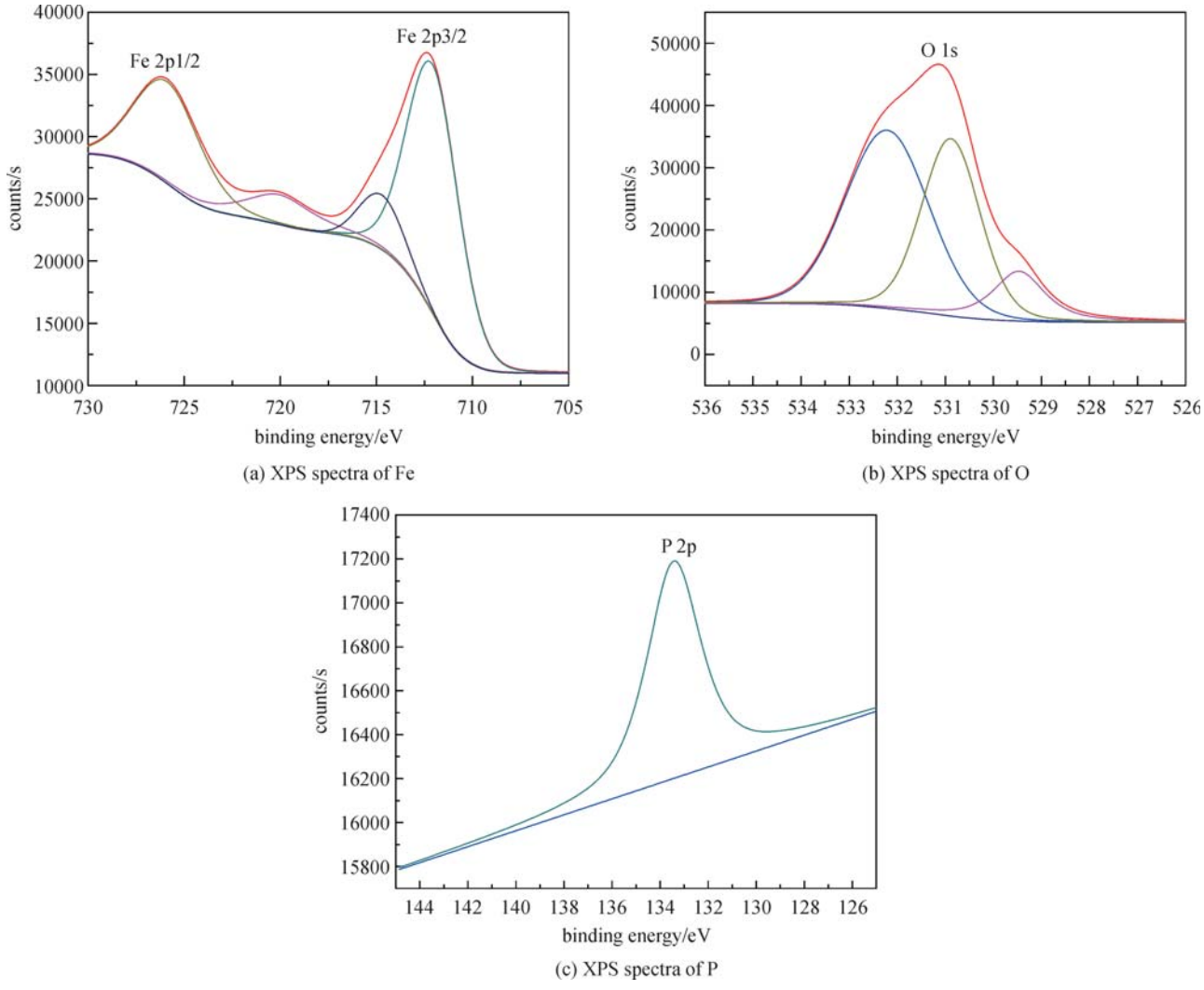

Fig. 6 XPS spectra of Fe, O, P, in R-nZVI after adsorption

Acknowledgements This research was supported by the Chinese National Special Science & Technology Project on Treatment and Control of Water Pollution (Nos. 2011ZX07301-002 and 2011ZX07213-001).

References

1. Erlk S. Experimental lakes in Canada. Science, 2008, 322(5906): 1316–1319
2. Schauser I, Chorus I, Heinzmann B. Strategy and current status of combating eutrophication in two Berlin lakes for safeguarding drinking water resources. Water Science and Technology, 2006, 54 (11–12): 93–100
3. Ding C C, Liu J. The state and impact factors of non-point source pollution in China. Chinese Population, Resource and Environment, 2011, 21(3): 86–89 (in Chinese)
4. Bai Y. 2010. Study on the pollution feature and treatment technology of rainwater runoff in Taihu New City, Wuxi. Dissertation for the Doctoral Degree. Beijing: Tsinghua University, 2011 (in Chinese)
5. Nurmi J T, Tratnyek P G, Sarathy V, Baer D R, Amonette J E, Pecher K, Wang C, Linehan J C, Matson D W, Penn R L, Driessen M D. Characterization and properties of metallic iron nanoparticles: spectroscopy, electrochemistry, and kinetics. Environmental Science & Technology, 2005, 39(5): 1221–1230
6. Li X Q, Elliott D W, Zhang W X. Zero-valent iron nanoparticles for abatement of environmental pollutants: materials and engineering aspects. Critical Reviews in Solid State and Material Sciences, 2006, 31(4): 111–122
7. Cao J S, Elliott D, Zhang W X. Perchlorate reduction by nanoscale iron particles. Journal of Nanoparticle Research, 2005, 7(4–5): 499–506
8. Cumbal L, Greenleaf J, Leun D, SenGupta A K. Polymer supported inorganic nanoparticles: characterization and environmental applications. Reactive & Functional Polymers, 2003, 4(1–3): 167–180
9. Metcalf E I. Wastewater Engineering-Treatment, Disposal, and Reuse. 3rd. New York: McGraw-Hill Incorporation, 1991
10. Gan L L, Zuo J E, Xie B M, Li P, Huang X. Zeolite (Na) modified by

nano-Fe particles adsorbing phosphate in rainwater runoff. Journal of Environmental Sciences (China), 2012, 24(11): 1929–1933

11. Zhang X, Lin S, Chen Z L, Megharaj M, Naidu R. Kaolinite-supported nanoscale zero-valent iron for removal of Pb^{2+} from aqueous solution: reactivity, characterization and mechanism. Water Research, 2011, 45(11): 3481–3488
12. Huang C P, Wang H W, Chiu P C. Nitrate reduction by metallic iron. Water Research, 1998, 35(8): 2257–2264
13. Boujelben N, Bouzid J, Elouear Z, Feki M, Jamoussi F, Montiel A. Phosphorus removal from aqueous solution using iron coated natural and engineered sorbents. Journal of Hazardous Materials, 2008, 151(1): 103–110
14. Duan J M, Lin J Q, Fang H D, Nie B, Wu J J, Wu G H. Experimental study on simultaneous removal of ammonium and phosphate in treated wastewater by modified zeolite. Chinese Journal of Environmental Engineering, 2009, 3(5): 829–833 (in Chinese)
15. Moulder J F, Stickle W F, Sobol P E. Handbook of X-ray Photoelectron Spectroscopy. Montreal: Perkin- Elmer Corporation Publisher, 1995
16. Sun Y P, Li X Q, Cao J S, Zhang W X, Wang H P. Characterization of zero-valent iron nanoparticles. Advances in Colloid and Interface Science, 2006, 120(1-3): 47–56